

# Detection of carboxylesterase 1 and carbamates with a novel fluorescent protein chromophore based probe

Jianan Dai<sup>a,1</sup>, Yu Zhao<sup>b,1</sup>, Yadan Hou<sup>a</sup>, Guoyan Zhong<sup>a</sup>, Rui Gao<sup>a</sup>, Jichun Wu<sup>a</sup>, Baoxing Shen<sup>a,\*</sup>, Xing Zhang<sup>a,\*\*</sup>

<sup>a</sup> School of Food Science and Pharmaceutical Engineering, Nanjing Normal University, Nanjing, Jiangsu, 210023, China

<sup>b</sup> Department of Food Science, Cornell University, Ithaca, NY, 14853, United States



## ARTICLE INFO

**Keywords:**  
 Carboxylesterase 1  
 Aggregation-induced emission  
 Fluorescent protein chromophore  
 Pesticide detection  
 Living cell imaging

## ABSTRACT

An aggregation-induced emission (AIE) fluorescent protein chromophore-based probe (CBZ-FP) for detection of human carboxylesterases (CESs) was designed and synthesized. CBZ-FP exhibited good cell permeability with a large stokes shift (116 nm) and can be applied to reveal the actual activities of CES1 in living cells associated with pesticides detoxification process. CBZ-FP can also serve as a fluorescence indicator of pesticide exposure in the way of hydrolyzing the carboxylic acid ester group in CBZ-FP. Therefore, CBZ-FP has high selectivity for CESs and can detect real-time activity of CES1 in biological samples. Molecular docking study was used to explore the binding of CESs and CBZ-FP. Finding that only one specific activity site of CESs can bind with probe. In view of the fact that, the biotransformation of drugs and poisons containing ester groups can carry out normally depending on CESs, Carboxylesterase probes are expected to contribute to the characterization of relevant disease.

## 1. Introduction

In the past decade, pesticides are used in agriculture worldwide to protect plants and crops from insects and pests infestations. Global agricultural production has also been greatly increased due to pesticides usage [1–3]. Carbamates, organophosphates are commonly used in agriculture [4–6] and they are hazardous to environment and human health [7–9]. Carbamate pesticides can irreversibly inhibit the activity of acetylcholinesterase in the central and peripheral nervous system [10, 11]. Therefore, it is crucial to develop a detection method towards carbamates [12,13].

Several methods have been developed to determine the pesticide residue, such as high performance liquid chromatography (HPLC), gas chromatography-mass spectrometry (GC/MS), electrochemical analysis, and enzyme-linked immunosorbent assays (ELISAs) [14–17]. However, these methods have many limitations, such as expensive instruments, complex sample pretreatment and the need for well-trained personnel [18,19], thus restricting their wide application in pesticide residue detection. Fluorogenic method [20,21], as a new approach in the field of

pesticides residue detection, attracts significant attentions due to simple operation, fast detection as well as high accuracy [22–24].

Fluorescent probes based on the inhibition of enzymes activity have shown satisfactory results for pesticide analysis [25,26]. As an important enzyme, carboxylesterase (CES) correlates with various biotransformation [27,28]. One important function of carboxylesterase1 (CES1) is to detoxify pesticides, therefore serving as an indicator for carbamates exposure [29]. However, developing probes for selective CES1 detection still represent a challenge [30,31].

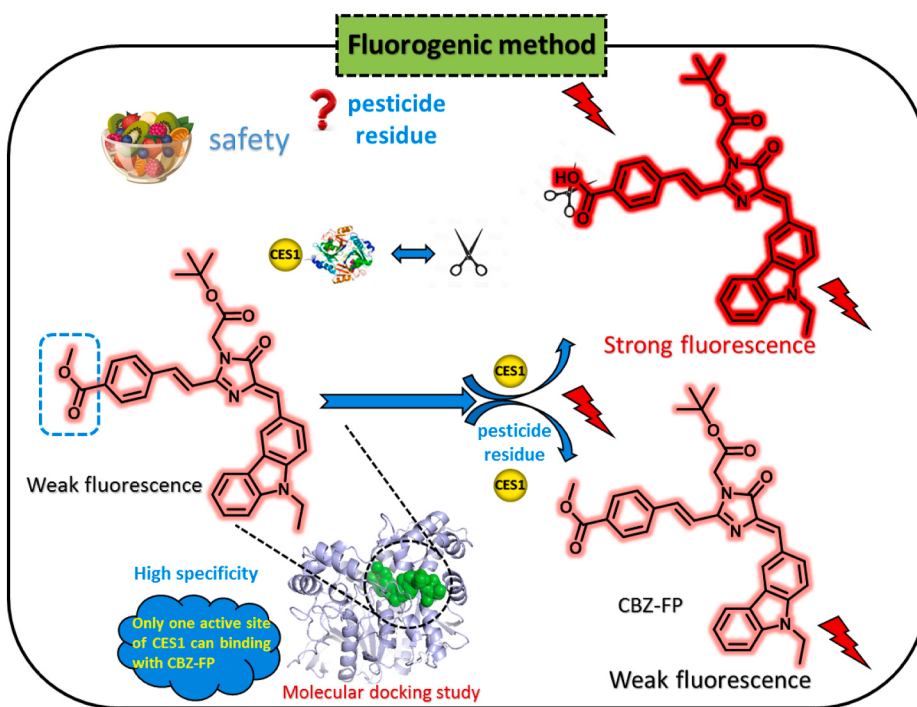
Herein, we designed an aggregation-induced emission (AIE) fluorescent probe functioning as a selective detector for CESs and carbaryl using fluorescent protein chromophore [32]. A red emission probe CBZ-FP (**Scheme 1**) was synthesized and applied to quantitative determine CES1 as well as carbaryl. The detection mechanism utilizing the hydrolysis of carboxylic acid ester group in CBZ-FP. Molecular docking study showed that only one specific activity site of CESs can bind with probe. CBZ-FP exhibits excellent stability over a broad pH range, and successfully carried out direct and dynamic detection on CES1 in living cells.

\* Corresponding author.

\*\* Corresponding author.

E-mail addresses: [shenbx@njnu.edu.cn](mailto:shenbx@njnu.edu.cn) (B. Shen), [zhangxing@njnu.edu.cn](mailto:zhangxing@njnu.edu.cn) (X. Zhang).

<sup>1</sup> They contribute equally to this work and should be considered as co-first author.



Scheme 1. Designing of probe CBZ-FP to detect carboxylesterase 1 and carbaryl.

## 2. Experimental

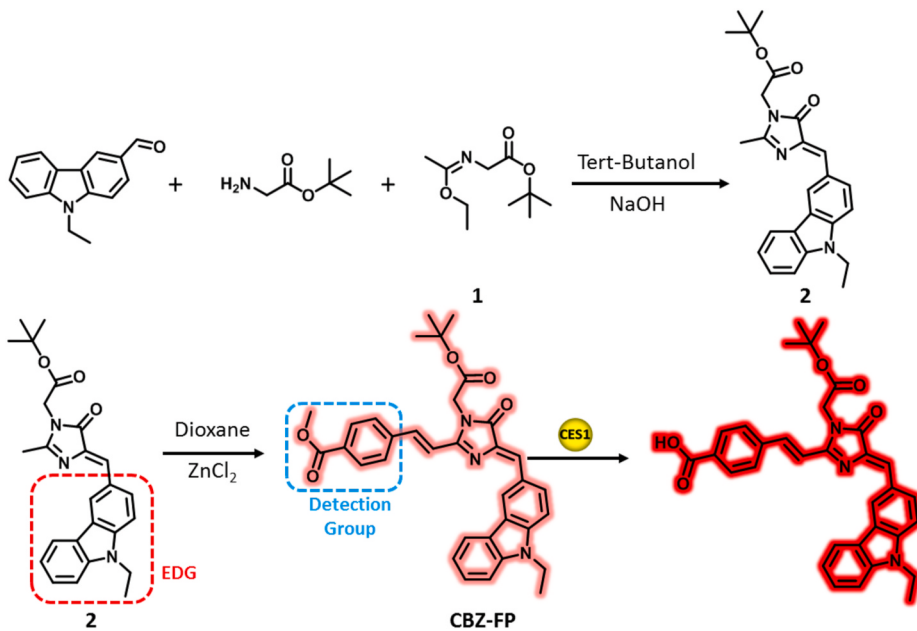
The synthesis and structural characterization of all compounds and were shown in supporting information.

**Fluorescence measurement CBZ-FP in glycerol mixture solutions:** CBZ-FP (10  $\mu$ M) were prepared in glycerol: MeOH mixture with increasing glycerol concentrations [33,34]. Fluorescence measurement was carried out using a fluorescence spectrometer (F97Pro19059) at excitation and emission wavelengths as indicated.

**Selectivity:** CBZ-FP (10  $\mu$ M) was added to 100 mM phosphate buffer (PBS, pH 7.4) and incubate at 37 °C for 3 min. After that, different enzymes including CES1, CES2, Hb, BSA, HSA, BuchE, lipase, papain,

lysozyme, chymotrypsin, proteinase K were put into the mixture to start the reaction [35,36]. The sources of all enzymes were shown in Table S16. The enzyme concentration was controlled to 50  $\mu$ g mL<sup>-1</sup>. The total volume of the enzyme reaction solution is 200  $\mu$ L and the content of DMSO is 1%. After incubating at 37 °C for 60 min, 200  $\mu$ L CH<sub>3</sub>CN was added to quench the reaction. Fluorescence measurement was carried out using a fluorescence microplate reader (Synergy H1) at excitation and emission wavelengths as indicated. All readings were normalized against the fluorescence intensity in the presence of CES1. Error bars: standard error ( $n = 3$ ).

**Titration experiment:** CBZ-FP (10  $\mu$ M) was added to 100 mM phosphate buffer (PBS, pH 7.4) and incubate at 37 °C for 3 min. After



Scheme 2. Synthesis of probe CBZ-FP.

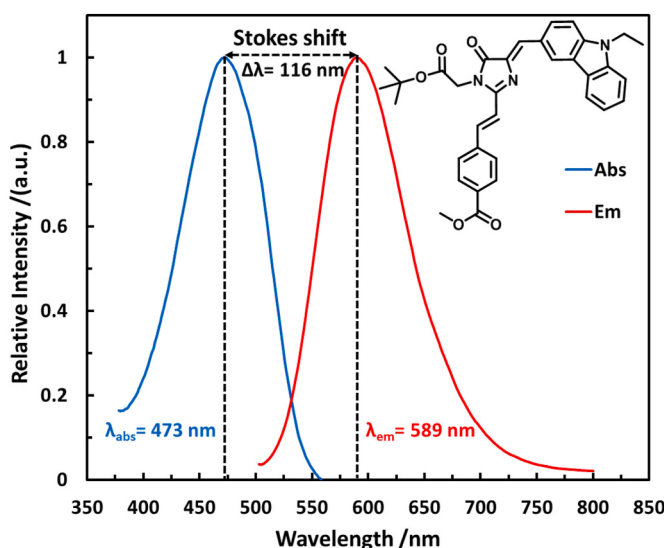


**Fig. 1.** Relative absorbance and fluorescence spectra of CBZ-FP (10  $\mu\text{M}$ ). Measured in  $\text{CH}_3\text{CN}/\text{PBS}$  buffer (v/v = 1/1) at 25 °C.

that, varying concentrations of CES1 was added and incubated for another 60 min. The total volume of the enzyme reaction solution is 200  $\mu\text{L}$ . Lastly, 200  $\mu\text{L}$   $\text{CH}_3\text{CN}$  was added to quench the reaction [37–39]. Fluorescence measurement was carried out using a fluorescence microplate reader (Synergy H1). Parameters for fluorescence measurement: ( $\text{Ex} = 473 \text{ nm}/\text{Em} = 589 \text{ nm}$ ). Error bars: standard error ( $n = 3$ ).

**Molecular docking study:** Lamarckian genetic algorithm in Auto-Dock 4.2 (Molecular Graphics Laboratory, La Jolla, CA, USA) was applied for molecular docking study. The structural information of CES1 was acquired from PDB data bank (PDB\_ID: 4AB1, resolution = 2.20 Å). The molecular docking study was performed between CBZ-FP and CES1 as well as other interfering proteins including CES2, Hb, BSA, HSA, BuchE, lipase, papain, lysozyme, chymotrypsin, proteinase K. The detailed information were shown in supporting information.

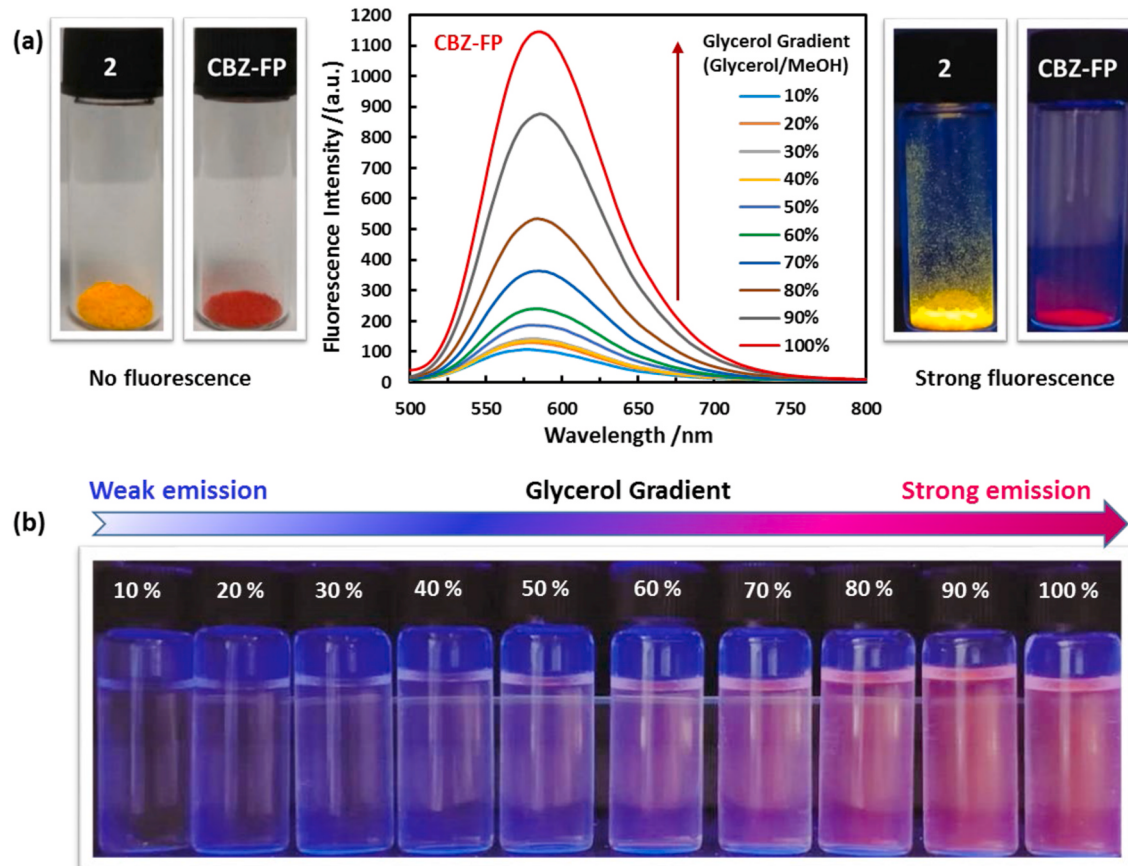
### 3. Results and discussion

#### 3.1. Construction of fluorescent protein chromophore mimic probe

Herein, an aggregation-induced emission (AIE) fluorescent protein chromophore (compound 2) was synthesized and used as the scaffold to design CESs selective probe CBZ-FP (Scheme 2). N-ethylcarbazole-3-carboxaldehyde was conjugated to the active methyl group of compound 2. The double bond between the carbazole and the fluorescent protein chromophore could twist. In aggregates, compound 2 and probe CBZ-FP exhibited strong yellow and red fluorescence, respectively. The twisting of double bond in compound 2 as well as probe CBZ-FP was restricted in solid state, and the energy was released in the form of light radiation. In probe CBZ-FP, the carboxylate ester group served as the specific reaction substrate of CESs.

#### 3.2. Spectroscopic response of CBZ-FP towards CES1

Here, The absorption and fluorescence spectrum of probe CBZ-FP was firstly measured. (Fig. 1). The maximum absorption wavelength

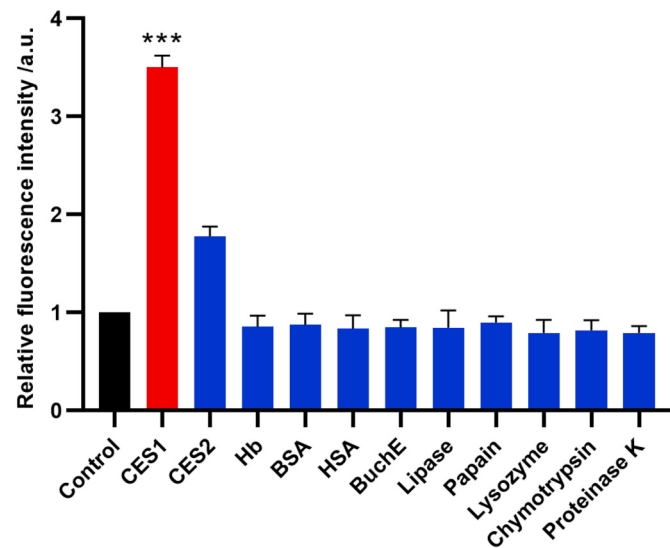
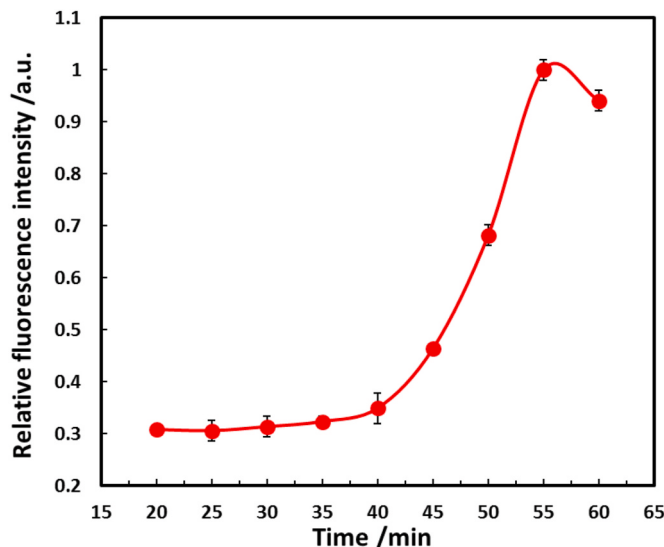


**Fig. 2.** Aggregation-induced emission properties. (a) Up inset: The fluorescence spectra of CBZ-FP (10  $\mu\text{M}$ ) in Glycerol and MeOH mixture with different glycerol concentrations; Fluorescence images of compound 2 and CBZ-FP in aggregates were obtained under ultraviolet lamp ( $\lambda_{\text{ex}} = 365 \text{ nm}$ ); (b) Bottom inset: the fluorescence images of CBZ-FP in various mixture solutions (Glycerol/MeOH) with different glycerol concentration.

**Table 1**

The photophysical properties of CBZ-FP.

Compounds	$\lambda_{\text{em}}^{\text{a}}$ (nm)	$\Phi^{\text{b}}$	$\lambda_{\text{abs}}^{\text{c}}$ (nm)	$\epsilon^{\text{d}}$ (M <sup>-1</sup> cm <sup>-1</sup> )	B <sup>e</sup> (M <sup>-1</sup> cm <sup>-1</sup> )	$\Delta\lambda^{\text{f}}$ (nm)
CBZ-FP	589	0.43	473	24504	10757	116

<sup>a</sup> Emission wavelength (nm).<sup>b</sup> Fluorescence quantum yield.<sup>c</sup> Absorbance wavelength (nm).<sup>d</sup> Molar extinction coefficient (M<sup>-1</sup>cm<sup>-1</sup>).<sup>e</sup> Brightness (B) (M<sup>-1</sup>cm<sup>-1</sup>).<sup>f</sup> Stokes shift (nm). The measurement of fluorescence quantum yield was showed in supporting information.**Fig. 3.** Relative fluorescence intensity of CBZ-FP incubated with various enzymes. The fluorescence intensity of control was normalized to 1.**Fig. 4.** Relative fluorescence intensity of CBZ-FP (10 μM) in the presence of CES1 (50 μg/mL) with different incubation time. Condition: V<sub>CH3CN</sub>/V<sub>PBS</sub> buffer (100 mM, pH 7.6) = 1/1,  $\lambda_{\text{ex}} = 473$  nm, the fluorescence intensity at 55 min was normalized to 1.

and corresponding maximum emission wavelength were determinate as 473 nm and 589 nm. Obviously, CBZ-FP has a remarkable Stokes shift (116 nm), which renders the probe low background noise upon

detecting biological samples. Interestingly, we found that CBZ-FP and its precursor have strong aggregation-induced emission (AIE) phenomenon. The AIE based fluorophore are insensitive to homogeneous system but become highly emissive in aggregate formation. Normally, fluorophore with AIE property are sensitive to microenvironmental changes including viscosity and water content in detection system. As shown in Fig. 2, under the excitation of ultraviolet light (365 nm), the solid of probe CBZ-FP as well as its precursor compound 2 exhibited strong red and yellow fluorescence, respectively. Thus, this fluorophore could be served as scaffold for designing selective AIE enzyme probe. The detail photophysical properties of CBZ-FP was listed in Table 1. In this work, during the detection process of CES1, the water content and viscosity of the detection system has no significant changes. Thus, the AIE properties of the probe almost have no impact on the detection of CES1.

We then tested the selectivity of CBZ-FP towards CES1 by monitoring the fluorescence intensity change when CBZ-FP was incubated with various commercial available enzymes. As shown in Fig. 3, no significant changes in fluorescence intensities could be observed when CBZ-FP was incubated with enzymes including CES1, CES2, Hb, BSA, HSA, BuchE, lipase, papain, lysozyme, chymotrypsin, proteinase K. However, the fluorescence intensity of CBZ-FP exhibited a significant enhancement ( $p < 0.05$ ) (3.5 fold) after incubating with CES1, which is induced by the hydrolysis of carboxylate group. The result indicate that CBZ-FP has good selectivity towards CESs. Fig. 4 showed that the fluorescence intensity of CBZ-FP increased with the increase of incubation time, possibly indicating that CBZ-FP slowly adopted to conformation enhancing fluorescence emission upon hydrolysis by CES1. In order to verify that the fluorescent response was due to CBZ-FP hydrolyzed by CES, we pretreated HepG-2 cells with a specific inhibitor of CES1 (UKA, UKA (3-O-(β-carboxy-ypropionyl)-ursolic acid)), before cell imaging was performed (Fig. S29). We further carried out density functional theory (DFT) calculation to explore HOMO-LUMO energy level of CBZ-FP as well as its hydrolysates (Figs. S19-S24). Classic CES1 inhibitors was used for selective validation, and found that bis-p-nitrophenyl phosphate (BNPP) and 3-O-(β-carboxy-ypropionyl)-ursolic acid (UKA) are effective in inhibiting the hydrolysis reaction (Fig. S27).

In order to explore the quantitative relationship between CBZ-FP and CESs, the titration experiment was carried out to acquire the sensitivity of CBZ-FP toward CES1. According to Fig. 5, the fluorescence intensity of CBZ-FP increased as a function of increasing CES1 concentration, and the fluorescence intensity gradually became a plateau as the concentration exceeded 50 μg/mL. The fluorescence intensity exhibited a good linear increasing trend when the concentration of CES1 increased from 0 to 50 μg/mL. A low detection limit (LOD) was calculated as (27.8 ng/mL) [40,41]. Detection limit measurement was showed in the supporting information. LOD was also compared with other reported work (Table S15). The results suggest that CBZ-FP could be employed to quantitatively determine CES1 with high selectivity.

### 3.3. Fluorescence response of CBZ-FP to pesticides

It is reported that organophosphates or carbamates pesticides can inhibit the activity of CES1 [29], therefore CBZ-FP can possibly serve as the indicator for organophosphates or carbamates pesticides. In fact, fluctuations in fluorescence intensity of CBZ-FP are due to the hydrolysis of carboxylic ester bond in CBZ-FP. We chose carbaryl as the target and conducted the concentration titration experiment [42–44]. As shown in Fig. 6, CES1 (5 μg/mL) was first pre-incubated at various carbaryl concentrations for 30 min, then CBZ-FP (10 μM) was added and together was further incubated for another 60 min.

Fig. 6a showed that with increasing carbaryl concentrations, the activity of CES1 was inhibited. However, the fluorescence intensity of CBZ-FP exhibited a decreasing tendency. Since, CES1 with high activities under the conditions of low carbaryl concentrations. At this time, the carboxylate group of the CBZ-FP was hydrolyzed, and the resulting intermediate has a carboxyl group, which provide the intermediate with

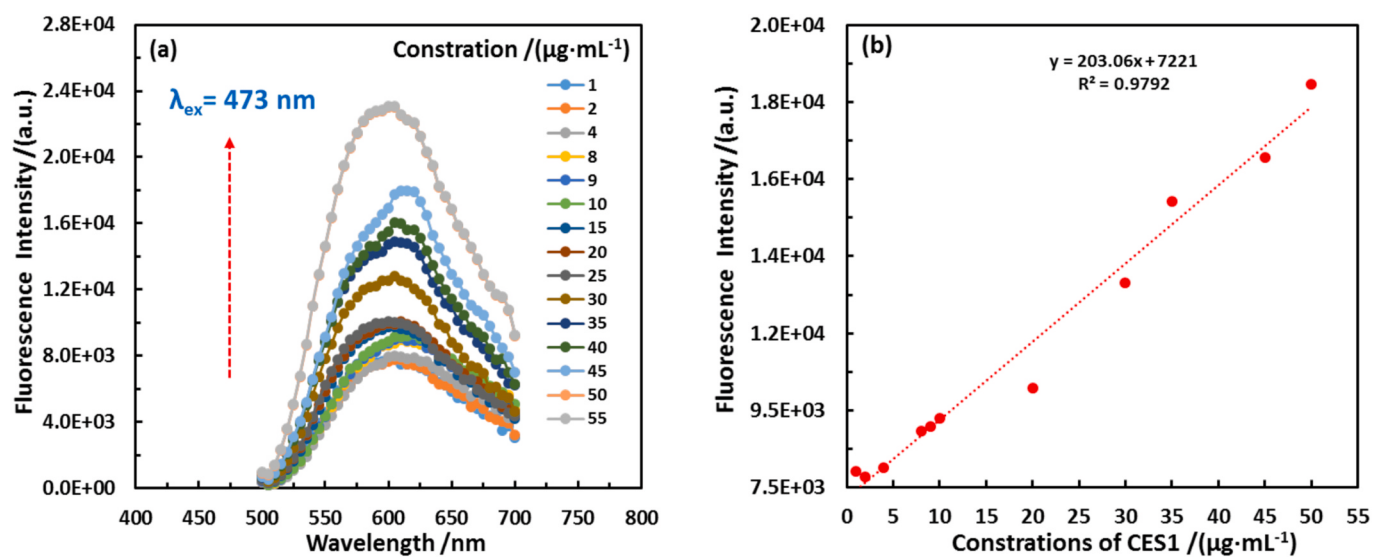


**Fig. 5.** (a) Emission spectra of CBZ-FP (10  $\mu\text{M}$ ) incubated with different concentrations of CES1; (b) Linear relationship between fluorescence intensity and CES1 concentrations. The measurement was performed at 37 °C.

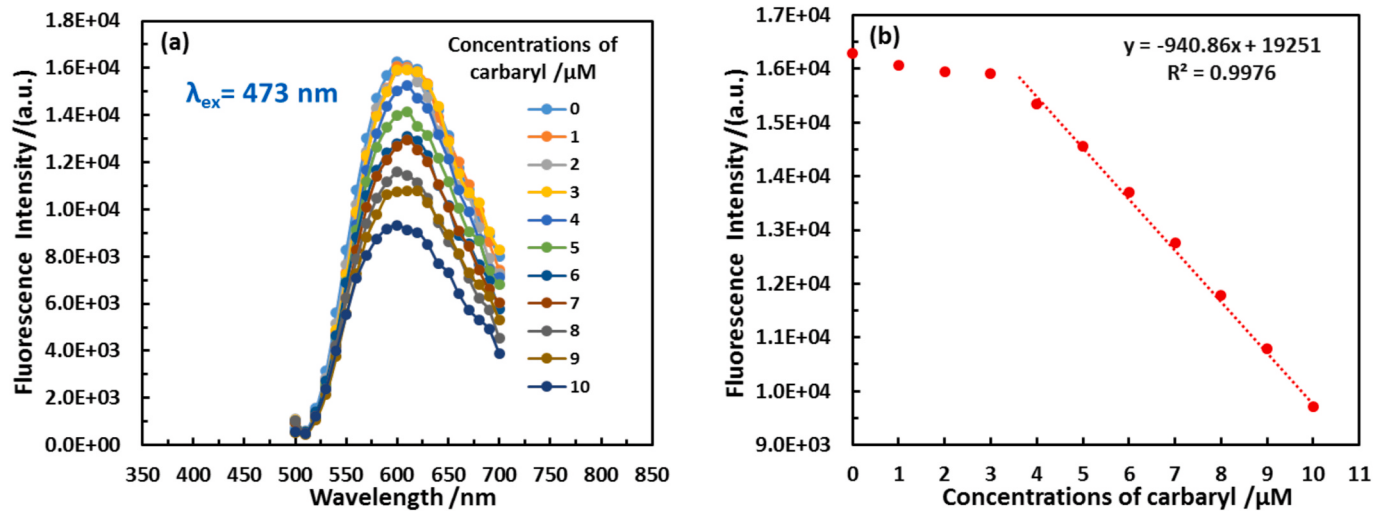


**Fig. 6.** (a) Emission spectra of CBZ-FP (10  $\mu\text{M}$ ) in CES1 (5  $\mu\text{g}/\text{mL}$ ) PBS buffer (pretreated with different concentrations of carbaryl for 30 min); (b) Fluorescence intensity at 589 nm versus carbaryl concentrations.

good water solubility and also enhance the fluorescence intensity. On the contrary, when the concentrations of carbaryl in a high level, the activity of CES1 was inhibited. At this time, CBZ-FP would not undergo a hydrolysis reaction, and thus the fluorescence intensity is relatively weak. It is easy to find from Fig. 6b that the fluorescence intensity of CBZ-FP is linear with carboxyl concentrations. The results of experiments demonstrated that CBZ-FP could be employed in quantitative detection of carbaryl residue.

#### 3.4. Molecular docking study and density functional theory (DFT) calculation

AlloSite was able to identify only one potential binding site in CES1, demonstrating as the green region in Fig. 7b. The pocket drug ability score is as high as 0.93 and solvent-accessible surface area is 1111.65 and 594.45, respectively. We then set up a docking cubic box with  $60 \times 60 \times 60$  step (step length: 0.375 Å) in the potential binding site region, allowing 200 times independent docking calculations for both CBZ-FP and hydrolyzed CBZ-FP, respectively. The result indicated that CBZ-FP

have a high affinity towards the potential binding site through both hydrophobic and hydrophilic forces (Fig. 7c). To further verify the high selectivity of CBZ-FP to CES1, molecular docking calculations were also performed between CBZ-FP and other interfering enzymes (Fig. 7d–m). As was shown in Table 2, the binding energy between CBZ-FP and CES1 under optimal conformational conditions as well as inhibit constant was lower than that between CBZ-FP and other interfering enzymes, which further demonstrated the high selectivity of CBZ-FP for CES1. The cluster analysis results of molecular docking study were displayed in Figs. S8–S18 and the hydrophobic interactions between CBZ-FP and other interfering enzymes were listed in Tables S2–S12. To verify the hydrolysate of CBZ-FP, the hydrolysate was isolated and purified via LC-MS for further verification, and the results proved that only methyl acetate group can be hydrolyzed by CES1 (Fig. S25). The changes of fluorescence and absorbance spectrums of CBZ-FP before and after metabolism was also provided in Fig. S26.

As the results shown in Fig. 8, the charge transfer transition did takes place in the A-π-D system of probe CBZ-FP, where methyl benzoate served as the electron acceptor group and carbazole group served as

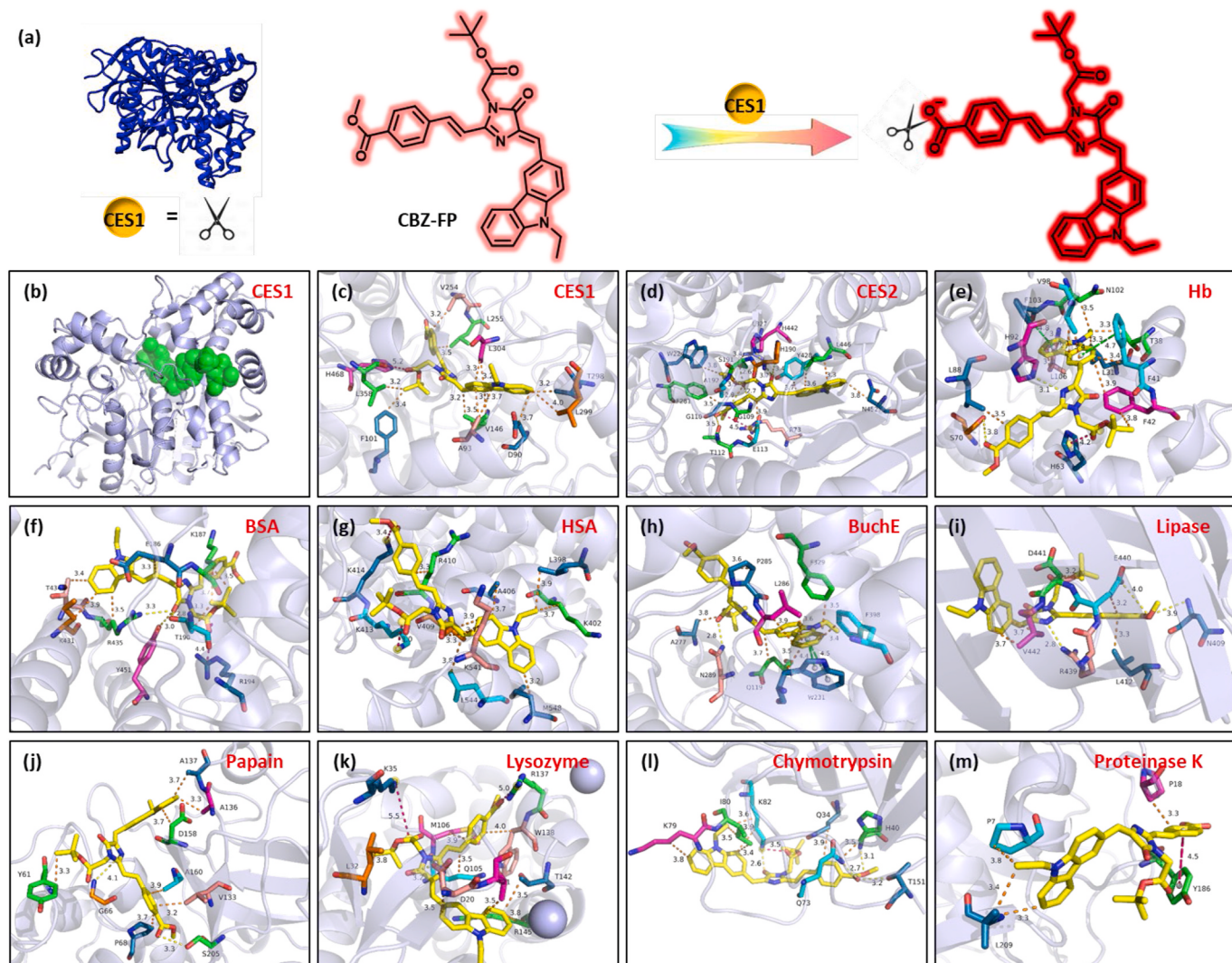


**Fig. 7.** (a) Detection process of CBZ-FP for CES1; (b) AlloSited predicted potential binding site (green color) in CES1 (PDB: 4AB1); (c–m) Interaction of CBZ-FP with CES1, CES2, Hb, BSA, HSA, BuchE, Lipase, Papain, Lysozyme, Chymotrypsin, Proteinase K. The PDB numbers of each enzyme were listed in Table S1. Yellow bonds indicates hydrogen bonding; orange bonds indicated hydrophobic interaction, green bonds indicate  $\pi$ -stacking interaction and pink ones are salt bridges.

**Table 2**  
Docking calculations between CBZ-FP and protein.

PDB	Binding Energy <sup>a</sup>	Inhibit constant <sup>b</sup>
CES1	-11.45	4.04 nM
CES2	-10.82	11.68 nM
Hb	-9.92	53.24 nM
BSA	-6.41	20.06 $\mu$ M
HSA	-8.76	377.22 nM
BuchE	-9.21	177.28 nM
Lipase	-5.7	65.93 $\mu$ M
Papain	-8.7	416.65 nM
Lysozyme	-9.28	158.16 nM
Chymotrypsin	-7.02	7.19 $\mu$ M
Proteinase K	-6.55	15.92 $\mu$ M

<sup>a</sup> Binding energy between CBZ-FP and protein under optimal conformational conditions.

<sup>b</sup> Inhibit constant between probe and protein.

electron donor group. It forms an electron “push-pull” interaction. However, when the probe CBZ-FP reacted with CES1, the carboxylic ester group was hydrolyzed to carboxylic group and formed the hydrolysates with carboxyl groups. In hydrolysates, the molecular dipole moment becomes larger, resulting in enhanced fluorescence of the

molecules in polar solvents. Besides, when the donating ability of the electron-donating group or withdrawing ability of the electron-withdrawing group is enhanced, the fluorescence will also be enhanced in A- $\pi$ -D system. In hydrolysates, carboxylic group enhance the withdrawing ability of the electron-withdrawing group. Thus, the fluorescence intensity of hydrolysates enhanced. However, the energy level difference between HOMO and LUMO orbitals of CBZ-FP did not change much before and after hydrolysis, thus the emission wavelength of fluorescent molecules almost has no changes before and after hydrolysis.

### 3.5. pH dependence

The pH stability of probe CBZ-FP is of great significance for practical applications because pH varies at a large range in food systems. Here, the fluorescence response of CBZ-FP in the presence of CES1 in PBS buffers with different pH was investigated (Fig. 9) and the results indicated no significant difference ( $p < 0.05$ ) in fluoresce intensity [45]. The fluorescence intensity of the PBS buffer with CBZ-FP only was further measured at different pH and the result still indicated no significant difference ( $p < 0.05$ ).

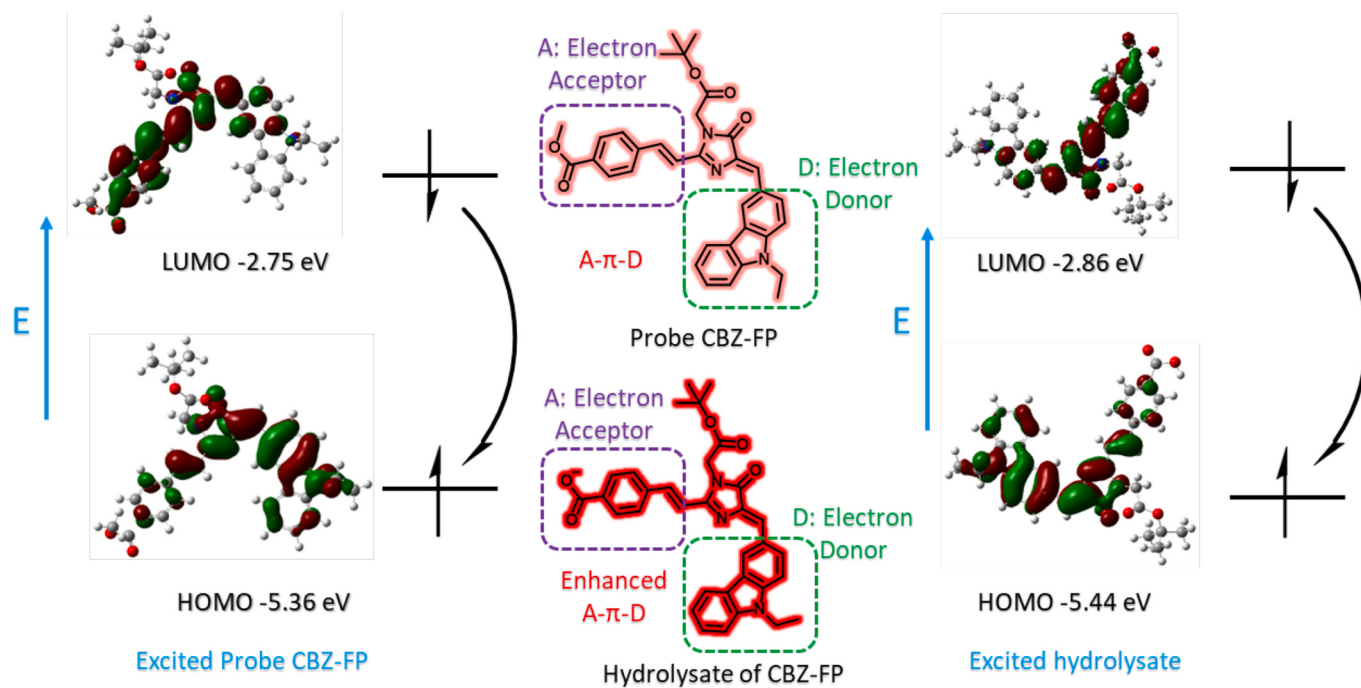


Fig. 8. Density functional theory (DFT) calculation of CBZ-FP and the hydrolysate of CBZ-FP.

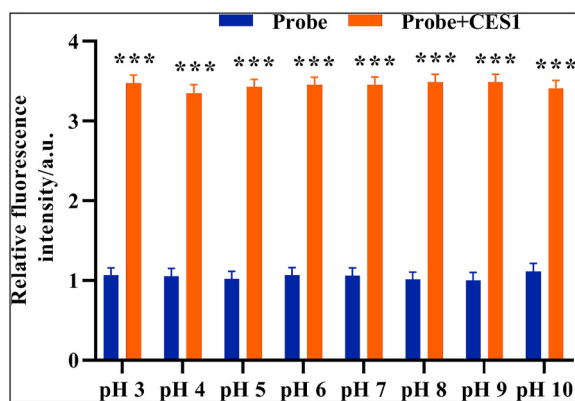
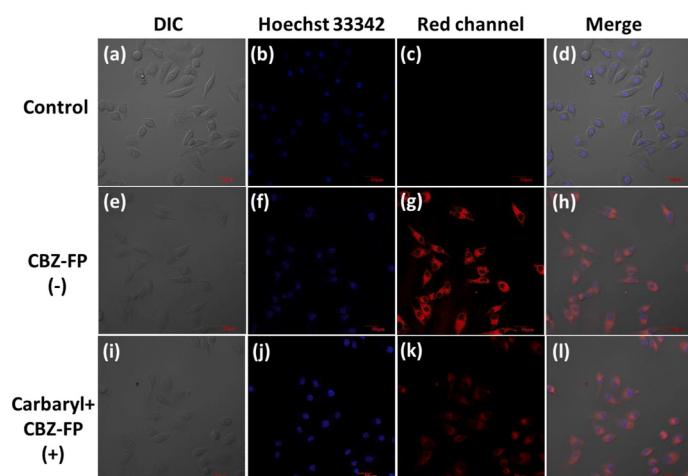


Fig. 9. Relative fluorescence intensity of CBZ-FP (10  $\mu$ M) in different pH buffer solution before and after incubated with CES1 (50  $\mu$ g/mL). The fluorescence intensity of CBZ-FP in pH 7.0 was normalized to 1.



### 3.6. Monitor the real-time activities of CES1 in living cells

CBZ-FP was further applied in living cells which performed as a real-time indicator to surveillance CES1 activity in HepG2 cells. Before applied in cell imaging, CBZ-FP has been tested to have low cytotoxicity, which indicated that CBZ-FP can be applied in living cells. (Fig. S1 was showed in supporting information). Fig. 10(a-d) was control and only HepG2 cells were incubated with nuclear dye Hoechst 33342. Fig. 10(e-h) was the experimental group, HepG2 cells was incubated with both CBZ-FP (10  $\mu$ M) and 10  $\mu$ M Hoechst 33342 for 30 min. After that, a red fluorescence signal was observed in red channel (Fig. 10g). However, on condition that HepG2 cells were pretreated with carbaryl (5  $\mu$ M) for 10 min, and then incubated with Hoechst 33342 (10  $\mu$ M) along with CBZ-FP (10  $\mu$ M) relatively for 30 min, the red fluorescence signal of HepG2 cells decreased (Fig. 10k) due to the activity of carboxylesterase was inhibited by carbaryl [46]. We further find that probe CBZ-FP exhibited low background fluorescence from the living cell images. All these results suggest that CBZ-FP is an excellent probe with great biocompatibility for revealing the real activity of CES1 in living cells.

Fig. 10. Living cell images of HepG2 cells. (a–c) HepG2 cells were stained by 10  $\mu$ M Hoechst 33342 for 30 min and imaging under the bright, blue and red channel, respectively; (d) Merge images (a), (b) and (c); (e–g) HepG2 cells were co-stained by 10  $\mu$ M Hoechst 33342 and 10  $\mu$ M CBZ-FP for 30 min and imaging under the bright, blue and red channel, respectively; (h) Merge images (e), (f) and (g); (i–k) HepG2 cells were incubated with 5  $\mu$ M carbaryl for 10 min firstly, and then co-stained with 10  $\mu$ M Hoechst 33342 as well as 10  $\mu$ M CBZ-FP for 30 min, then imaging under the bright, blue and red channel, respectively; (l) Merge images (i), (j) and (k); (m) The average intensity of images in red channel. Scale bar = 30  $\mu$ m.

#### 4. Conclusion

In a word, we constructed an AIE probe (CBZ-FP) for selectively detecting the CESs. The twisting of the double bond between the carbazole and the fluorescent protein chromophore rendered CBZ-FP and its precursor compound 2 strong AIE phenomenon. For the entire fluorescent probe, the ester group is the recognition group and the carbazole is the fluorescent group. The fluorescent group was excited before the ester group reacted with the carboxylesterase, the excited electrons cannot transition to the ground state, so that the fluorescence of the fluorescent group was blocked. After the ester group was hydrolyzed to a carboxyl group, the electronegativity is greatly enhanced as well as the fluorescence. CBZ-FP has minimal background noise due to its large Stokes shift (116 nm). CBZ-FP has excellent membrane permeability and can serve as a real-time indicator to surveillance CESs activity in HegG2 cells. CBZ-FP can be further used for quantitative detection of carbaryl. A low detection limit (LOD) was calculated as (27.8 ng/mL). Therefore, CBZ-FP is one of the few developed fluorescent probes that can selectively detect both CES1 and carbaryl in biological samples. This study sets up a practical platform for the further exploration of CESs associated physiological and pathological process.

#### CRediT authorship contribution statement

**Jianan Dai:** Writing – original draft. **Yu Zhao:** Writing – original draft. **Yadan Hou:** Data curation. **Guoyan Zhong:** Data curation. **Rui Gao:** Formal analysis. **Jichun Wu:** Formal analysis. **Baoxing Shen:** Writing – review & editing, Supervision. **Xing Zhang:** Writing – review & editing, Supervision.

#### Declaration of competing interest

The authors declare that they have no known competing financial interests or personal relationships that could have appeared to influence the work reported in this paper.

#### Acknowledgements

This work was financially supported by the “Youth Program of National Natural Science Foundation” of China (Grant No. 22007048), Natural Science Foundation of the Jiangsu Higher Education Institutions of China (20KJB150046), Science and Technology Innovation Project for Overseas Students of Nanjing in 2020 (184080H201148), Jiangsu innovation and entrepreneurship doctoral program to Baoxing Shen.

#### Appendix A. Supplementary data

Supplementary data to this article can be found online at <https://doi.org/10.1016/j.dyepig.2021.109444>.

#### References

- [1] Yang L, Liu YL, Liu CG, Ye F, Fu Y. Two luminescent dye@MOFs systems as dual-emitting platforms for efficient pesticides detection. *J Hazard Mater* 2020;381:120966.
- [2] Shi J, Deng Q, Li Y, Zheng M, Chai Z, Wan C, et al. A rapid and ultrasensitive tetraphenylethylene-based probe with aggregation-induced emission for direct detection of alpha-amylase in human body fluids. *AnalChem* 2018;90(22):13775–82.
- [3] Nile SH, Kim DH, Nile A, Park GS, Gansukh E, Kai G. Probing the effect of quercetin 3-glucoside from Dianthus superbus L against influenza virus infection- *in vitro* and *in silico* biochemical and toxicological screening. *Food Chem Toxicol: Int J Publ Br Indus Biol Res Assoc* 2020;135:110985.
- [4] Wu Z, Du Y, Zhou Q, Chen L. One pot solvothermal synthesis of novel fluorescent phloem-mobile phenylpyrazole amide pesticides fused olefin moieties to enhance insecticidal bioactivities and photodegradation properties. *Pestic Biochem Physiol* 2020;163:51–63.
- [5] Yu Y, Luo X, Wang X, Sun Z, Song C, You J. A novel high-performance liquid chromatography-fluorescence analysis coupled with *in situ* degradation derivatization technique for quantitation of organophosphorus thioester pesticide residues in tea. *Anal Bioanal Chem* 2018;410(26):6911–22.
- [6] Yan X, Li H, Hu T, Su X. A novel fluorimetric sensing platform for highly sensitive detection of organophosphorus pesticides by using egg white-encapsulated gold nanoclusters. *Biosens Bioelectron* 2017;91:232–7.
- [7] Champagne P-L, Kumar R, Ling C-C. Multi-responsive self-assembled pyrene-appended  $\beta$ -cyclodextrin nanoaggregates: discriminative and selective ratiometric detection of pirimicarb pesticide and trinitroaromatic explosives. *Sensor Actuator B Chem* 2019;281:229–38.
- [8] Lin B, Yan Y, Guo M, Cao Y, Yu Y, Zhang T, et al. Modification-free carbon dots as turn-on fluorescence probe for detection of organophosphorus pesticides. *Food Chem* 2018;245:1176–82.
- [9] Yan X, Song Y, Zhu C, Li H, Du D, Su X, et al. MnO<sub>2</sub> nanosheet-carbon dots sensing platform for sensitive detection of organophosphorus pesticides. *AnalChem* 2018;90(4):2618–24.
- [10] Huang S, Yao J, Chu X, Liu Y, Xiao Q, Zhang Y. One-step facile synthesis of nitrogen-doped carbon dots: a ratiometric fluorescent probe for evaluation of acetylcholinesterase activity and detection of organophosphorus pesticides in tap water and food. *J Agric Food Chem* 2019;67(40):11244–55.
- [11] Liu L, Sun C, Yang J, Shi Y, Long Y, Zheng H. Fluorescein as a visible-light-induced oxidase mimic for signal-amplified colorimetric assay of carboxylesterase by an enzymatic cascade reaction. *Chem Eur J* 2018;24(23):6148–54.
- [12] Chen H, Hu O, Fan Y, Xu L, Zhang L, Lan W, et al. Fluorescence paper-based sensor for visual detection of carbamate pesticides in food based on CdTe quantum dot and nano ZnTPyP. *Food Chem* 2020;327:127075.
- [13] Qin S-J, Yan B. A facile indicator box based on Eu<sup>3+</sup> functionalized MOF hybrid for the determination of 1-naphthol, a biomarker for carbaryl in urine. *Sensor Actuator B Chem* 2018;259:125–32.
- [14] Luo M, Wei J, Zhao Y, Sun Y, Liang H, Wang S, et al. Fluorescent and visual detection of methyl-paraoxon by using boron-and nitrogen-doped carbon dots. *Microchem J* 2020;154:104547.
- [15] Tseng M-H, Hu C-C, Chiu T-C. A fluorescence turn-on probe for sensing thiocarb using rhodamine B functionalized gold nanoparticles. *Dyes Pigments* 2019;171:107674.
- [16] Nsibande SA, Forbes PB. Fluorescence detection of pesticides using quantum dot materials - a review. *Anal Chim Acta* 2016;945:9–22.
- [17] Wang X, Hou T, Dong S, Liu X, Li F. Fluorescence biosensing strategy based on mercury ion-mediated DNA conformational switch and nicking enzyme-assisted cycling amplification for highly sensitive detection of carbamate pesticide. *Biosens Bioelectron* 2016;77:644–9.
- [18] Nagaboooshanam S, John AT, Wadhwa S, Mathur A, Krishnamurthy S, Bharadwaj LM. Electro-deposited nano-webbed structures based on polyaniline/multi walled carbon nanotubes for enzymatic detection of organophosphates. *Food Chem* 2020;323:126784.
- [19] Lu L, Su H, Liu Q, Li F. Development of a luminescent dinuclear Ir(III) complex for ultrasensitive determination of pesticides. *AnalChem* 2018;90(19):11716–22.
- [20] Dai J, Ma C, Zhang P, Fu Y, Shen B. Recent progress in the development of fluorescent probes for detection of biothiols. *Dyes Pigments* 2020;177:108321.
- [21] Ma C, Zhong G, Zhao Y, Zhang P, Fu Y, Shen B. Recent development of synthetic probes for detection of hypochlorous acid/hypochlorite. *Spectrochim Acta Mol Biomol Spectrosc* 2020;240:118545.
- [22] Zhang F, Liu Y, Ma P, Tao S, Sun Y, Wang X, et al. A Mn-doped ZnS quantum dots-based ratiometric fluorescence probe for lead ion detection and “off-on” strategy for methyl parathion detection. *Talanta* 2019;204:13–9.
- [23] Shen B, Zhu W, Zhi X, Qian Y. A lysosome targeting probe based on fluorescent protein chromophore for selectively detecting GSH and Cys in living cells. *Talanta* 2020;208:120461.
- [24] Zhang C, Jiang Z, Jin M, Du P, Chen G, Cui X, et al. Fluorescence immunoassay for multiplex detection of organophosphate pesticides in agro-products based on signal amplification of gold nanoparticles and oligonucleotides. *Food Chem* 2020;326:126813.
- [25] Chang J, Li H, Hou T, Li F. Paper-based fluorescent sensor for rapid naked-eye detection of acetylcholinesterase activity and organophosphorus pesticides with high sensitivity and selectivity. *Biosens Bioelectron* 2016;86:971–7.
- [26] Crow JA, Borazjani A, Potter PM, Ross MK. Hydrolysis of pyrethroids by human and rat tissues: examination of intestinal, liver and serum carboxylesterases. *Toxicol Appl Pharmacol* 2007;221(1):1–12.
- [27] Liu Z-m, Du H-j, Wang T-q, Ma Y-n, Liu J-r, Yan M-c, et al. Selective and sensitive detection and quantification of human carboxylesterase 1 by a ratiometric fluorescence probe. *Dyes Pigments* 2019;171:107711.
- [28] Tian Z, Ding L, Li K, Song Y, Dou T, Hou J, et al. Rational design of a long-wavelength fluorescent probe for highly selective sensing of carboxylesterase 1 in living systems. *AnalChem* 2019;91(9):5638–45.
- [29] Li D, Li Z, Chen W, Yang X. Imaging and detection of carboxylesterase in living cells and zebrafish pretreated with pesticides by a new near-infrared fluorescence off-on probe. *J Agric Food Chem* 2017;65(20):4209–15.
- [30] Bencharit S, Edwards CC, Morton CL, Howard-Williams EL, Kuhn P, Potter PM, et al. Multisite promiscuity in the processing of endogenous substrates by human carboxylesterase 1. *J Mol Biol* 2006;363(1):201–14.
- [31] Li D, Li Z, Chen W, Yang X. Imaging and detection of carboxylesterase in living cells and zebrafish pretreated with pesticides by a new near-infrared fluorescence off-on probe. *J Agric Food Chem* 2017;65(20):4209–15.
- [32] Chen S, Hong Y, Liu J, Tseng NW, Liu Y, Zhao E, et al. Discrimination of homocysteine, cysteine and glutathione using an aggregation-induced-emission-active hemicyanine dye. *J Mater Chem B* 2014;2(25):3919–23.

- [33] Liu J, Xiong WH, Ye LY, Zhang WS, Yang H. Developing a novel nanoscale porphyrinic metal-organic framework: a bifunctional platform with sensitive fluorescent detection and elimination of nitenpyram in agricultural environment. *J Agric Food Chem* 2020;68(20):5572–8.
- [34] Qi L, Wu W, Kang Q, Hu Q, Yu L. Detection of organophosphorus pesticides with liquid crystals supported on the surface deposited with polyoxometalate-based acetylcholinesterase-responsive supramolecular spheres. *Food Chem* 2020;320:126683.
- [35] Bala R, Dhingra S, Kumar M, Bansal K, Mittal S, Sharma RK, et al. Detection of organophosphorus pesticide – malathion in environmental samples using peptide and aptamer based nanoprobe. *Chem Eng J* 2017;311:111–6.
- [36] Shen B, Wang LF, Zhi X, Qian Y. Construction of a red emission BODIPY-based probe for tracing lysosomal viscosity changes in culture cells. *Sensor Actuator B Chem* 2020;304:127271.
- [37] Dong Y, Zheng W, Chen D, Li X, Wang J, Wang Z, et al. Click reaction-mediated T2 immunosensor for ultrasensitive detection of pesticide residues via brush-like nanostructure-triggered coordination chemistry. *J Agric Food Chem* 2019;67(35):9942–9.
- [38] Wu X, Song Y, Yan X, Zhu C, Ma Y, Du D, et al. Carbon quantum dots as fluorescence resonance energy transfer sensors for organophosphate pesticides determination. *Biosens Bioelectron* 2017;94:292–7.
- [39] Liang P, Cao Y, Dong Q, Wang D, Zhang, Jin S, et al. A balsam pear-shaped CuO SERS substrate with highly chemical enhancement for pesticide residue detection. *Mikrochim Acta* 2020;187(6):335.
- [40] Wang J, Chen Q, Tian N, Zhu W, Zou H, Wang X, et al. A fast responsive, highly selective and light-up fluorescent probe for the two-photon imaging of carboxylesterase in living cells. *J Mater Chem B* 2018;6(11):1595–9.
- [41] Qu F, Wang H, You J. Dual lanthanide-probe based on coordination polymer networks for ratiometric detection of glyphosate in food samples. *Food Chem* 2020;323:126815.
- [42] Jiang M, Chen C, He J, Zhang H, Xu Z. Fluorescence assay for three organophosphorus pesticides in agricultural products based on Magnetic-Assisted fluorescence labeling aptamer probe. *Food Chem* 2020;307:125534.
- [43] Cheng SC, Lee RH, Jeng JY, Lee CW, Shiea J. Fast screening of trace multiresidue pesticides on fruit and vegetable surfaces using ambient ionization tandem mass spectrometry. *Anal Chim Acta* 2020;1102:63–71.
- [44] Carullo P, Chino M, Cetrangolo GP, Terreri S, Lombardi A, Manco G, et al. Direct detection of organophosphate compounds in water by a fluorescence-based biosensing device. *Sensor Actuator B Chem* 2018;255:3257–66.
- [45] Duan H, Ding Y, Huang C, Zhu W, Wang R, Xu Y. A lysosomal targeting fluorescent probe and its zinc imaging in SH-SY5Y human neuroblastoma cells. *Chin Chem Lett* 2019;30(1):55–7.
- [46] Wen Y, Huo F, Yin C. Organelle targetable fluorescent probes for hydrogen peroxide. *Chin Chem Lett* 2019;30(10):1834–42.